LANGMUIR

Article

pubs.acs.org/Langmuir

Line Tension and Wettability of Nanodrops on Curved Surfaces

Shantanu Maheshwari, Martin van der Hoef, and Detlef Lohse*,†

Physics of Fluids, Department of Science and Technology, Mesa+ Institute, and J. M. Burgers Centre for Fluid Dynamics, University of Twente, P. O. Box 217, 7500 AE, Enschede, The Netherlands

†Max Planck Institute for Dynamics and Self-Organization, 37077, Göttingen, Germany

ABSTRACT: In this work we study the formation of nanodrops on curved surfaces (both convex and concave) by means of molecular dynamics simulations, where the particles interact via a Lennard-Jones potential. We find that the contact angle is not affected by the curvature of the substrate, in agreement with previous experimental findings. This means that the change in curvature of the drop in response to the change in curvature of the substrate can be predicted from simple geometrical considerations, under the assumption that the drop's shape is a spherical cap, and that the volume remains unchanged through the curvature. The resulting prediction is in perfect agreement with the simulation results, for both convex and concave substrates. In addition, we calculate the line tension, namely, by fitting the contact angle for different size drops to the modified Young equation. We find that the line tension for concave surfaces is larger than for convex surfaces, while for zero curvature it has a clear maximum. This feature is found to be correlated with the number of particles in the first layer of the liquid on the surface.

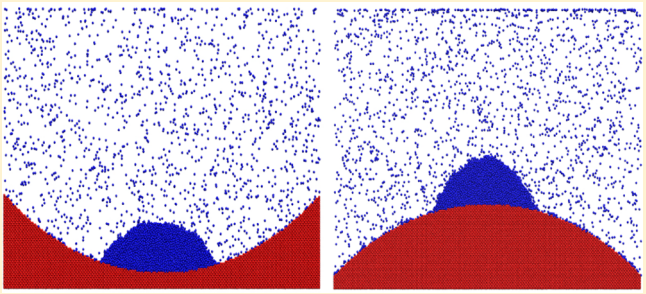

INTRODUCTION

The line tension is a key property for understanding the behavior of nanodrops and, thereby, of great technological relevance for lithography techniques or in micro- and nanofluidics.[1−4] On *curved* surfaces the line tension is of great significance for froth floatation, microporous solid, and condensation on nanorods.[5] Due to the small magnitude of line tension, it can affect wetting properties at the nanoscale without having any effect on the micro- or macroscale. Understanding, and hence predicting, the line tension of nanodrops is nontrivial. Although there have been a number of theoretical and experimental studies on the subject, up to recently there was no consensus even on the sign nor on the order of magnitude.[6]

The concept of line tension was introduced more than a century ago by Gibbs,[7] who concluded that interactions at the three-phase contact line cannot be explained by surface free energies of each pair of phases alone. He defined the line tension as the excess free energy per unit length of a contact line of three phases, analogous to surface tension, which is the excess free energy per unit area. In 1937, Harkins[8] managed to theoretically calculate the order of magnitude of line tension from the relation between latent heat of vaporization and the free, latent, and total energy of the three-phase contact line. In 1977, Pethica[1] defined line tension for a liquid drop on an ideal solid surface. He included the line tension in the conditions for equilibrium in the free energy expression, which when minimized with respect to the contact angle at constant volume, gives the so-called modified Young equation:

$$\cos\theta = \frac{\gamma_{SV} - \gamma_{SL}}{\gamma_{LV}} - \frac{\tau/\gamma_{LV}}{R} = \cos\theta_Y - \frac{\tau/\gamma_{LV}}{R} \quad (1)$$

where θ is the contact angle and R is the radius of curvature of the contact circle of the liquid drop on an ideal (chemically and geometrically homogeneous) solid surface when it is in equilibrium with its own vapor, as illustrated in Figure 1. In eq 1, τ is the line tension, θ_Y is Young contact angle, and γ_{SL}, γ_{SV}, and γ_{LV} are the solid−liquid, solid−vapor, and liquid−vapor

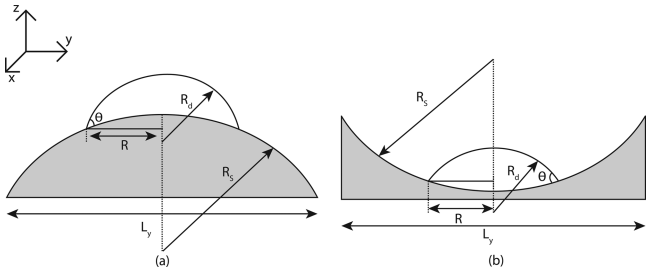

Figure 1. Definition of the various geometrical parameters used in this work, for (a) the convex surface and (b) the concave surface. Three different radii of curvatures can be identified: radius of surface curvature (R_S), radius of drop curvature (R_d), and radius of curvature of the contact line (R). Note that we define R_S such that for the convex surface it has a positive value and for the concave surface a negative value.

Received: October 23, 2015
Revised: December 4, 2015
Published: December 11, 2015

DOI: 10.1021/acs.langmuir.5b03925
Langmuir 2016, 32, 316−321

surface tensions, respectively. In eq 1, we have not considered the effect of curvature of the liquid−vapor interface on the surface tension,[9] because if these effects become comparable in magnitude to the line tension, then the measured τ cannot be considered as "pure" line tension, but as an apparent line tension.[6,10]

The magnitude of the line tension has been calculated from the free energy associated with the three-phase contact line using density functional theory[11,12] or a model based on the interface displacement.[13,14] Most of these theoretical analyses predict a value of the line tension in the range of 10^{-12} to 10^{-11} N. Experimental investigations show that the order of magnitude of an effective line tension varies from 10^{-5} to 10^{-12} N with both positive and negative signs,[2,6,15−19] which basically only shows how challenging it is to measure the line tension experimentally. The primary reason for this variation is the contact angle hysteresis caused by surface heterogeneities, either geometric or chemical, which are always present for an actual experimental situation. But also the extremely low size range of the drops makes it very difficult to measure the line tension experimentally. For example, in the case of water drops with a surface tension of 0.072 N/m and a line tension of 10^{-11} N (the most consistent order of magnitude reported in literature), the line tension becomes significant only for contact line curvatures of around 5 nm.[20]

Studies have not been confined to flat surfaces. Extrand and Moon[21] have investigated the dependence of contact angle on surface curvatures experimentally, however for drop sizes in the micro- and millimeter range. Marmur and Krasovitski[22] have calculated the line tension on spherical surfaces from theoretical calculations, but it lacks validation from experimental or simulation data.

Apart from theoretical and experimental research, there have also been a number of studies on the line tension and measurement of contact angle using molecular dynamics simulations.[23−26] Such simulations have the advantage that the line tension can be calculated with relatively large accuracy, and also the heterogeneities can be well-controlled. Shi and Dhir[24] studied the behavior of the contact angle of drops on a plane solid substrate as a function of temperature and force field parameters, using a simple Lennard-Jones model (as described in the next section), as well as a more advanced model potential for water. Ingebrigtsen and Toxvaerd[25] have calculated the contact angles for drops of different sizes and observed that the contact angle from MD simulations disagrees with the Young contact angle for nanodrops which have a very small contact angle. Weijs et al.[23] have analyzed the effect of line tension by measuring contact angles of droplets on a plane substrate by varying the droplet size and found that the line tension decreases with increasing θ_Y.

In the present work, we have extended the simulation by Weijs et al.[23] to curved substrates. Simulations have been performed in 3D, that is, for spherical drops, and in quasi-2D (where one dimension is considerably smaller than the other two), to which we refer as cylindrical drops. Cylindrical drops give the value of θ_Y as the contact line is free from any curvature and hence the contact angle does not change with the size of the drop. The effect of the curvature on the contact line can then be predicted by calculating the contact angle for spherical drops of different sizes and comparing it with θ_Y. In this way, we have systematically studied the effect of surface curvature on the magnitude of the line tension and wettability of nanodrops on curved surfaces.

NUMERICAL METHOD

Molecular Dynamics Simulations of Nanodrops. Molecular dynamics (MD) simulations were performed to simulate the drop on a solid substrate for which we used the open source code GROMACS.[27] Two kinds of particles were used in the simulations: solid substrate particles, which are held fixed in a fcc lattice setting during the whole simulation, and liquid/vapor particles, which are free to move and in the equilibrium-state form in a liquid drop on the solid substrate, with a vapor phase filling the remaining volume. The interaction between the particles is described by Lennard-Jones potential:

$$\phi_{ij}^{LJ}(r) = 4\epsilon_{ij}\left[\left(\frac{\sigma_{ij}}{r}\right)^{12} - \left(\frac{\sigma_{ij}}{r}\right)^{6}\right] \quad (2)$$

in which ϵ_{ij} is the interaction strength between particles i and j and σ_{ij} is the characteristic size of particles, which is set to a value $\sigma = 0.34$ nm for all interactions. The potential is truncated at a relatively large cutoff radius of $r_c = 5\sigma$. The time step for updating the particle velocities and positions was set at $dt = \sigma\sqrt{(m/\epsilon_{LL})}/400$, where m is the mass of the particles and $\epsilon_{LL} = 3$ kJ/mol is the Lennard-Jones interaction parameter for the liquid phase. Simulations have been performed in an *NVT* ensemble where the temperature is fixed at 300 K, which is below the critical point for the Lennard-Jones parameters (σ, ϵ_{LL}) that we have used. Periodic boundary conditions have been employed in all three directions. We have studied two different kinds of systems to examine the effect of line tension: quasi-2D and 3D. In quasi-2D, the system size in one dimension is substantially less than the size of the system in the other two dimensions. The typical dimension of the system is 10.5σ in the x-direction and around 150σ in the y- and z-directions, where the x-, y-, and z directions are defined in Figure 1. In 3D, the system size in all three directions is of the same order of magnitude. The system size is such that in all cases the distance between a drop and its neighboring image is at least 80σ. In all simulations, the overall number density is kept constant. The equilibrium contact angle (or wettability) of the liquid drop on the solid substrate was varied by changing the interaction strength between solid and liquid particles (ϵ_{SL}), from 1.0 to 2.0 kJ/mol. In all simulations the liquid drop was found to be in equilibrium with its own vapor, where the liquid and vapor density was found to be in close agreement with the theoretical result as obtained from the equation of state of the Lennard-Jones fluid.[28]

In the simulations, the line tension is evaluated in terms of the tension length (l) defined as $l = -\tau/\gamma_{LV}$, which is of the order of magnitude of the molecular scale. We have calculated the magnitude of the line tension length along the lines of Weijs et al.,[23] by measuring the equilibrium θ for different size drops and fitting a straight line to $\cos\theta$ vs $1/R$, where the slope is then equal to l. Repeating these calculations for various values of the LJ parameters then gives the tension length ($-\tau/\gamma_{LV}$) as a function of θ_Y.

Two kinds of surface curvatures were used in this study as shown in Figure 2: a curved outward (or convex) surface defined as a positive curvature and a curved inward (or concave) surface defined as a negative curvature. In order to keep the overall number density constant, we have scaled the system dimensions while increasing the number of particles in the simulations. We have also scaled the radius of curvature of the surface according to the system dimensions. The surface curvature scales with $n^{1/2}$ in the case of quasi-2D and with $n^{1/3}$ in the case of 3D, where n is the number of moving particles in the simulation. Note that owing to the discrete nature of particles and the relatively small system size, the curvature of the solid substrate is not smooth but consists of steps, with a step height equal to the particle diameter, as shown in Figure 2. Because of these finite steps, the three-phase contact line will be in contact with different crystallographic axes in each simulation. Different crystallographic axes exhibit different surface energies which may lead to a slight change in the contact angle.[29,30] We have ignored this effect as we have averaged the contact angle for different equilibrium profiles which means that the contact angle calculated from our simulations is average over different crystallographic axes. We have also ignored the effect of surface

DOI: 10.1021/acs.langmuir.5b03925
Langmuir 2016, 32, 316−321

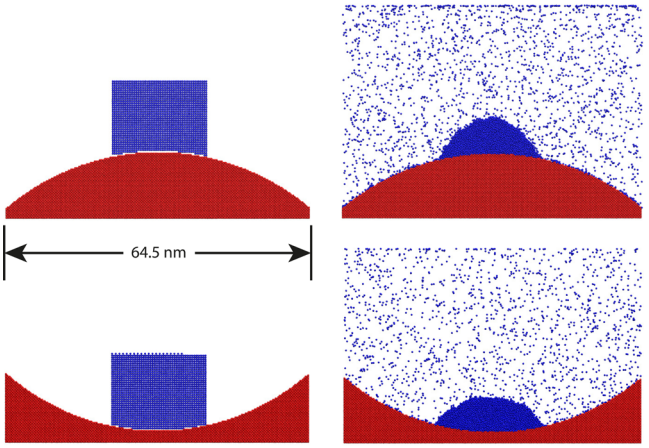

Figure 2. Example of the initial configuration (left) and the final steady-state configuration (right) after 5×10^7 time steps of the nanodrop simulations for convex (top) and concave (bottom) surfaces.

reconstruction as solid particles remain fixed in an fcc lattice during the whole simulation. This occurs either with less stable metal surfaces, semiconductor surfaces at very high temperatures, or polymer surfaces with polar groups.[31−33] We are not dealing with polar polymer groups or high temperatures, so it is justified to ignore this effect.

Initially, the liquid particles are set in a fcc configuration close to the solid substrate and free to move from then on at the prescribed temperature (see Figure 2). After equilibrium has been reached, i.e., after around 5×10^7 time steps, the density field is calculated by averaging over typically 1,000,000 time steps (which corresponds to roughly 2 ns) taking into account the fluctuation of the center of mass of the droplet. The radius of curvature of the droplet is then obtained by fitting a sphere (circle in 2D) to the isodensity contour of 0.5 of the normalized density field, $\rho^*(r)$, defined as $\rho^*(r) = \frac{\rho(r) - \rho_V}{\rho_L - \rho_V}$, where ρ_V and ρ_L is the bulk vapor and liquid density, respectively. Since the liquid very near to the solid substrate is subject to layering, we have excluded the density field in the range of 2σ from the substrate for the circular cap fitting. From the intersection of the circular fit with the substrate, the contact angle and volume of the drop are evaluated (see Figure 3). Note that we have split the time interval over which we

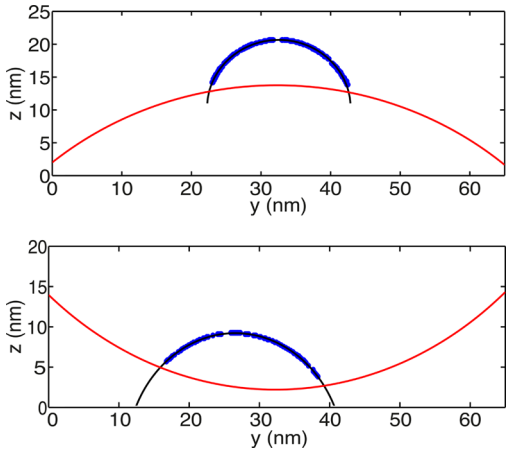

Figure 3. Example of a circular cap fit (black line) to the isodensity contour of 0.5 (points) for a drop on a convex and a concave surface of constant curvature. The drops can freely shift on the surface due to the statistical fluctuations. In particular, in the concave case the left shift as compared to the initial situation (Figure 2, bottom left) is apparent.

measured into 10 subsets and calculated the average of each subset in order to evaluate a standard deviation, from which the error bars in the results of Figures 4, 5, and 6 were obtained.

RESULTS AND DISCUSSION

Wettability of Cylindrical Nanodrops on Curved Surfaces. Figure 4 shows the Young contact angle as a

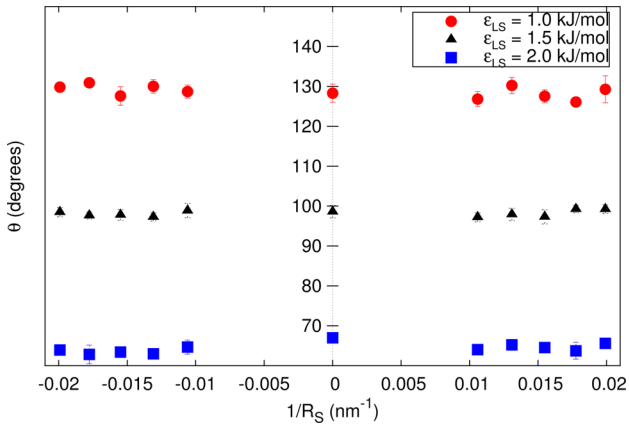

Figure 4. Contact angle (θ) of the nanodrop on a solid substrate as a function of surface curvature ($1/R_S$).

function of the surface curvature, for three different values of the liquid−solid interaction strength. It can be clearly seen that the contact angle is unaffected by the surface curvature, which is consistent with the experimental observations by Extrand and Moon[21] for microscopic drops. Note that Wolansky and Marmur[34] also showed theoretically that the contact angle is independent of the shape of the surface, unless line tension is considered. This means that curvature effects are only prominent in nanoscale systems where the line tension is appreciable as shown in the next section. Figure 5 shows that

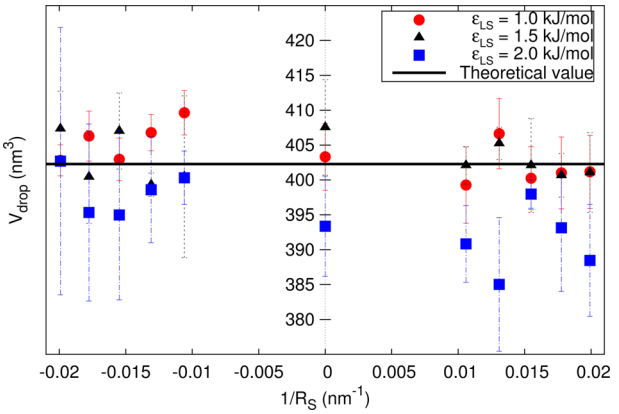

Figure 5. Volume of the nanodrop on a solid substrate as a function of surface curvature ($1/R_S$).

also the drop volume does not change with the surface curvature, which is expected since the volume is set by the condition of liquid−vapor equilibrium, which to first order is not affected by the surface curvature. In fact, the straight line in Figure 5 is the volume of the liquid drop evaluated from the bulk vapor−liquid equilibrium calculated from a highly accurate equation of state of the LJ fluid for the given temperature and overall number density.[28] The slight difference with the volume

DOI: 10.1021/acs.langmuir.5b03925
Langmuir 2016, 32, 316−321

as found in the simulations could be attributed to the effect of the liquid−vapor surface and the solid substrate, which are not accounted for in bulk phase equilibrium. Figure 6 shows the

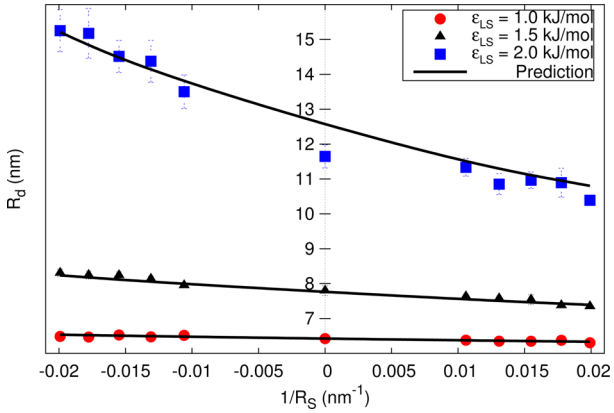

Figure 6. Radius of curvature, (R_d) of the nanodrop on a solid substrate as a function of surface curvature $(1/R_S)$.

variation of the radius of drop curvature (R_d) with surface curvature $(1/R_S)$. The simulation results are found to be in very good agreement with the prediction for R_d that follows from straightforward geometric relations for the drop volume as a function of the contact angle and surface curvature. In this, we take the volume of the drop as calculated from the equation of state, and the contact angle for a planar surface as reference values.

Line Tension of Nanodrops on Curved Surfaces. The line tension of LJ nanodrops has been calculated by fitting the modified Young equation, eq 1, to the simulation data. To this end, different sized LJ drops were simulated in 3D on the curved surface, and the cosine of the contact angle is plotted against the inverse of the radius of the curvature of the three-phase contact line, $1/R$, as shown in Figure 7. The slope of the straight line fitted through the data points then gives the line tension length $l = -\tau/\gamma_{LV}$. To double check, in Figure 7, we also show the result for cos θ for the quasi-2D system (cylindrical

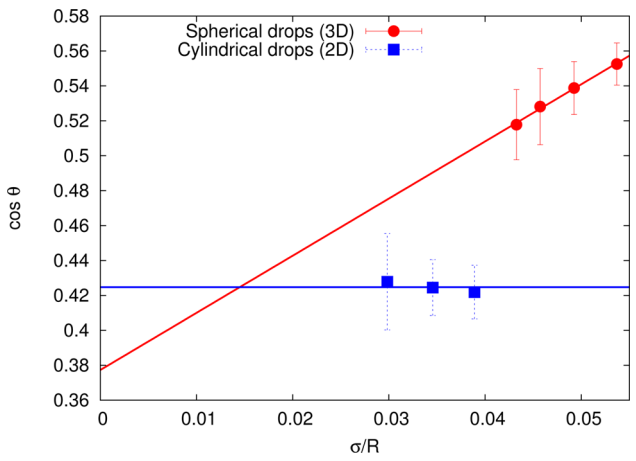

Figure 7. Results from the simulation for the contact angle on a concave surface with $V_{drop}^{1/3}/R_S = -0.2$ as a function of the curvature of the base circles (σ/R). The circles are the results for spherical drops, while the squares are for cylindrical drops. Straight lines are the linear fit through the data points. The slope of the straight line for spherical drops gives the line tension length $l = -\tau/\gamma_{LV}$.

drop), which as expected is not changing with the curvature of the drop because the contact line is free of any curvature and the line tension does not have any effect on it. According to eq 1, the two lines in Figure 7 should intersect at zero surface curvature. However, we find a small offset, which can most likely be contributed to the fact that the exact position of the liquid−vapor interface is not well-defined. That is, there is a smooth transition between the two distinct phases and many logical definitions are available to calculate the position of the interface. Hence quantities which are derived from the interface location, such as contact angle, volume, and radius of curvature of the drop, etc., will slightly vary depending on the definition,[6] which may result in a slight offset from eq 1. Note also that, for these typical values of the contact angle, only a slight error in θ of say 1% leads to errors of 3% in cos θ, which leads even to larger errors in the extrapolated value of the line fit.

Figure 8 shows the magnitude of the line tension length as a function of the surface curvature normalized by $V_{drop}^{1/3}$, where

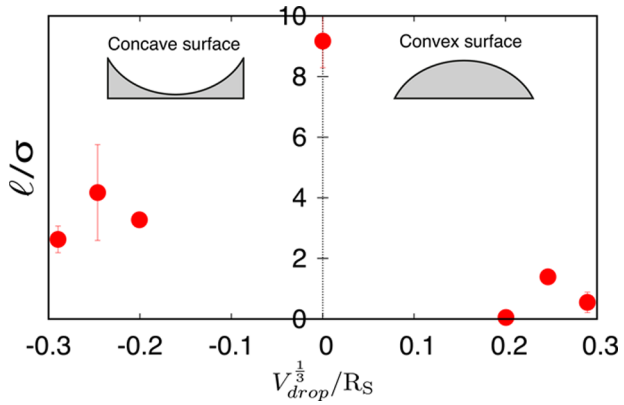

Figure 8. Variation of l as a function of $V_{drop}^{1/3}/R_S$. Note that smaller moduli of $V_{drop}^{1/3}/R_S$ are not possible due to the graininess of the surface particles.

V_{drop} is the volume of the drop as calculated from the equation of state for Lennard-Jones fluid.[28] We find a clear maximum in the case of the planar surface which is compatible with the theoretical predictions;[22,34] however, surprisingly we find that l is much higher in the case of concave surfaces (negative curvature) as compared to convex surfaces (positive curvature). From Figure 8, we can infer that the magnitude of the surface curvature does not have a very strong effect on the line tension length but it is strongly dependent on the sign of the surface curvature. We investigated this finding by analyzing the arrangement of particles very close to the surface. In Figure 9, we have plotted the variation of density of particles and the absolute number of particles in a drop as a function of distance from the surface. Both quantities are evaluated from the time-averaged number of particles for concentric spherical shells or layers of thickness 0.1σ. The variation in the absolute number of particles is determined by averaging the number of particles in each layer over time. Density in each layer is then calculated by dividing the absolute number of particles in each layer by the volume of that layer. It can be seen that the amplitude of the oscillations in the density is much larger in the case of the planar surface as compared to the curved ones, yet the difference in density oscillations between positive and negative surface curvature is small. However, the variation in the number of particles in the drop as a function of distance from the surface clearly shows the difference between the three types of

DOI: 10.1021/acs.langmuir.5b03925
Langmuir 2016, 32, 316−321

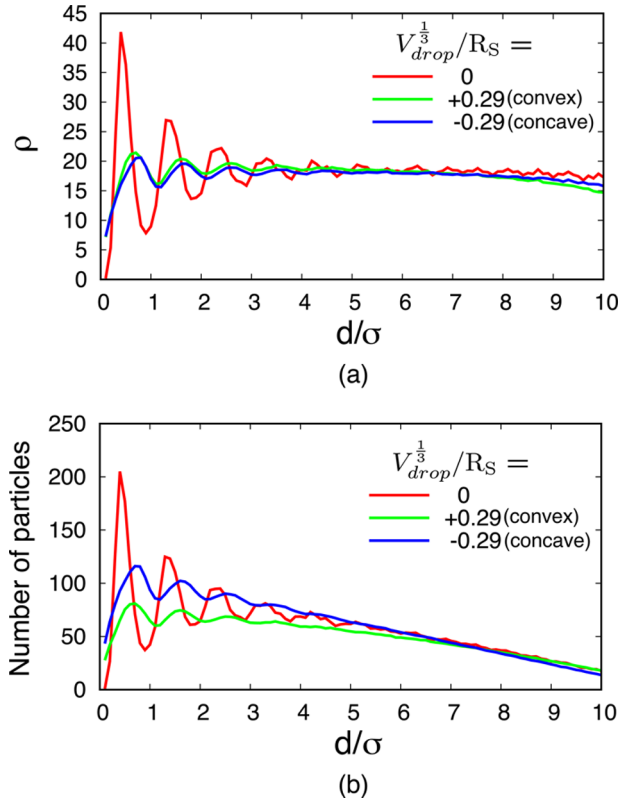

Figure 9. (a) Density and (b) absolute number of particles in the drop as a function of distance from the surface. Density of particles is calculated by dividing the absolute number of particles by the volume of each layer.

surfaces. The amplitude of the first peak is maximal in the case of a flat surface, then followed by the peak of negative and positive surface curvature, respectively. This trend is directly correlated with the magnitude of the line tension length, which suggest that more particles in layers close to the surface imply a larger line tension. Note that the absolute number of particles and the density of particles as a function of distance are related to each other by the volume of each layer. Since the density of particles is almost the same for both curvatures, this implies that the volume of layers very close to the surface is larger in the case of a concave surface. We have also analyzed the structure of the particles very near to the surface by evaluating radial distribution functions or pair correlation functions for particles in the first two layers as shown in Figure 10. The magnitude of the second peak in the radial distribution function is marginally larger in the case of curved surfaces as compared to the plane surface, but there is no difference between positive

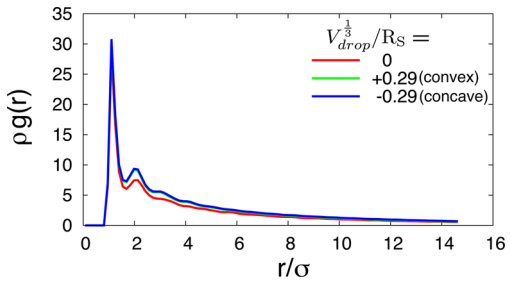

Figure 10. Radial distribution function of particles within two layers from the surface.

and negative surface curvatures which indicates that it is the absolute number of particles in the layers near to the surface which is responsible for the decrease in magnitude of the line tension and not the relative arrangement of the particles. From Figure 11, we can see a direct proportionality between the line

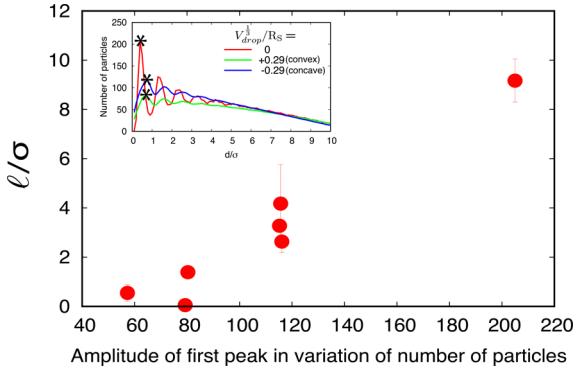

Figure 11. Amplitude of the first peak in oscillations of variation of number of particles as a function of the distance from the surface plotted against the magnitude of the line tension length for various surface curvatures. The asterisk in inset shows the peaks which are plotted in the graph.

tension length and the amplitude of the first oscillation of a variation of of number of particles with the distance from the surface.

The actual quantity of interest, the line tension, can be calculated by multiplying the line tension length by the liquid–vapor surface tension (γ_{LV}). Kirkwood and Buff[35] showed that the latter can be calculated by integrating the difference between normal and tangential components of the pressure tensor across the interface,

$$\gamma_{LV} = \frac{1}{2}\int_0^{L_z} [p_n(z) - p_t(z)]\, dz \quad (3)$$

We have used this procedure to calculate γ_{LV} from independent molecular dynamics simulation of liquid molecules in equilibrium with its own vapor and for a planar interface. Note that the factor 1/2 in eq 3 is the correction for the extra interface that is present due to periodic boundary conditions. We again emphasize that we have not considered surface tension as a function of interface curvature. The radius of curvature of a nanodrop of 7 nm is required to change the surface tension by 5% for the Lennard-Jones particles that we are simulating.[9,36] The radius of curvature of drops in our simulations is in the range of 10 nm. So the assumption of constant surface tension is fairly acceptable. For our Lennard-Jones parameters, i.e., ϵ_{LL} = 3.0 kJ/mol, this procedure gave a value of γ_{LV} = 4.1893 × 10^{-3} N/m. Using this value for the surface tension, the order of magnitude of the line tension is coming in the vicinity of 10^{-12} N which is very close to the theoretical prediction and many experimental findings.[2,6,11,13,19] The maximum value of the line tension is around 13 × 10^{-12} N for planar surface, and the minimum value is 0.07 × 10^{-12} N, which is almost zero, in the case of a convex surface.

CONCLUSIONS

Molecular dynamics simulations were performed for liquid drops on curved surfaces. The Young contact angle was found to be constant with surface curvature which is consistent with previous experimental and theoretical predictions. The volume

DOI: 10.1021/acs.langmuir.5b03925
Langmuir 2016, 32, 316–321

of the drop is also found to be independent of the curvature of the surface, and the radius of curvature of the drop is well-predicted by simple geometric relations by keeping contact angle and volume constant. The magnitude of the line tension is calculated by MD simulation and found to be comparable with theoretical values. The line tension strongly depends on the sign of the surface curvature: its value is much larger in the case of negative curvature (concave surface) as compared to positive curvature (convex surface), while it reaches a maximum for zero curvature. This trend is found to be correlated with the number of particles in the initial layers of the drop. The relative arrangement of particles near the surface is found to be the same which means that the number of particles near the three-phase contact line is the only significant factor which is responsible for altering the magnitude of the line tension on curved surfaces.

AUTHOR INFORMATION

Corresponding Author

*E-mail: d.lohse@utwente.nl.

Notes

The authors declare no competing financial interest.

ACKNOWLEDGMENTS

We thank Joost Weijs for useful discussions and help with MD simulations using GROMACS and SURFsara, NWO for providing computational facilities for the simulations, and FOM for financial support.

REFERENCES

(1) Pethica, B. A. The Contact Angle Equilibrium. *J. Colloid Interface Sci.* **1977**, *62*, 567−569.

(2) Amirfazli, A.; Neumann, A. W. Status of the three-phase line tension. *Adv. Colloid Interface Sci.* **2004**, *110*, 121−141.

(3) Peters, R. D.; Yang, X. M.; Kim, T. K.; Sohn, B. H.; Nealey, P. F. Using Self-Assembled Monolayers Exposed to X-rays To Control the Wetting Behavior of Thin Films of Diblock Copolymers. *Langmuir* **2000**, *16*, 4625−4631.

(4) Lopes, W. A.; Jaeger, H. M. Hierarchical self-assembly of metal nanostructures on diblock copolymer scaffolds. *Nature* **2001**, *414*, 735−738.

(5) He, J.; Zhang, Q.; Gupta, S.; Emrick, T.; Russell, T. P.; Thiyagarajan, P. Drying Droplets: A Window into the Behavior of Nanorods at Interfaces. *Small* **2007**, *3*, 1214−1217.

(6) Schimmele, L.; Napiòrkowski, M.; Dietrich, S. Conceptual aspects of line tensions. *J. Chem. Phys.* **2007**, *127*, 164715.

(7) Gibbs, J. W. *The collected works of J. W. Gibbs*; Yale University Press: New Haven, CT, USA, 1957.

(8) Harkins, W. D. Linear or Edge Energy and Tension as Related to the Energy of Surface Formation and of Vaporization. *J. Chem. Phys.* **1937**, *5*, 135−140.

(9) Tolman, R. C. The Effect of Droplet Size on Surface Tension. *J. Chem. Phys.* **1949**, *17*, 333−337.

(10) Schimmele, L.; Dietrich, S. Line tension and the shape of nanodroplets. *Eur. Phys. J. E: Soft Matter Biol. Phys.* **2009**, *30*, 427−430.

(11) Getta, T.; Dietrich, S. Line tension between fluid phases and a substrate. *Phys. Rev. E: Stat. Phys., Plasmas, Fluids, Relat. Interdiscip. Top.* **1998**, *57*, 655−671.

(12) Bauer, C.; Dietrich, S. Quantitative study of laterally inhomogeneous wetting films. *Eur. Phys. J. B* **1999**, *10*, 767−779.

(13) Dobbs, H. T.; Indekeu, J. O. Line tension at wetting: interface displacement model beyond the gradient-squared approximation. *Phys. A* **1993**, *201*, 457−481.

(14) Churaev, N.; Starov, V.; Derjaguin, B. The shape of the transition zone between a thin film and bulk liquid and the line tension. *J. Colloid Interface Sci.* **1982**, *89*, 16−24.

(15) Gaydos, J.; Neumann, A. The dependence of contact angles on drop size and line tension. *J. Colloid Interface Sci.* **1987**, *120*, 76−86.

(16) Li, D.; Neumann, A. Determination of line tension from the drop size dependence of contact angles. *Colloids Surf.* **1990**, *43*, 195−206.

(17) Amirfazli, A.; Kwok, D.; Gaydos, J.; Neumann, A. Line Tension Measurements through Drop Size Dependence of Contact Angle. *J. Colloid Interface Sci.* **1998**, *205*, 1−11.

(18) Heim, L.-O.; Bonaccurso, E. Measurement of Line Tension on Droplets in the Submicrometer Range. *Langmuir* **2013**, *29*, 14147−14153.

(19) Marmur, A. Line Tension and the Intrinsic Contact Angle in Solid−Liquid−Fluid Systems. *J. Colloid Interface Sci.* **1997**, *186*, 462−466.

(20) Lohse, D.; Zhang, X. Surface nanobubbles and nanodroplets. *Rev. Mod. Phys.* **2015**, *87*, 981−1035.

(21) Extrand, C. W.; Moon, S. I. Contact Angles on Spherical Surfaces. *Langmuir* **2008**, *24*, 9470−9473.

(22) Marmur, A.; Krasovitski, B. Line Tension on Curved Surfaces: Liquid Drops on Solid Micro- and Nanospheres. *Langmuir* **2002**, *18*, 8919−8923.

(23) Weijs, J. H.; Marchand, A.; Andreotti, B.; Lohse, D.; Snoeijer, J. H. Origin of line tension for a Lennard-Jones nanodroplet. *Phys. Fluids* **2011**, *23*, 022001.

(24) Shi, B.; Dhir, V. K. Molecular dynamics simulation of the contact angle of liquids on solid surfaces. *J. Chem. Phys.* **2009**, *130*, 034705.

(25) Ingebrigtsen, T.; Toxvaerd, S. Contact Angles of Lennard-Jones Liquids and Droplets on Planar Surfaces. *J. Phys. Chem. C* **2007**, *111* (24), 8518−8523.

(26) Halverson, J. D.; Maldarelli, C.; Couzis, A.; Koplik, J. Atomistic simulations of the wetting behavior of nanodroplets of water on homogeneous and phase separated self-assembled monolayers. *Soft Matter* **2010**, *6*, 1297−1307.

(27) Hess, B.; Kutzner, C.; van der Spoel, D.; Lindahl, E. GROMACS 4: Algorithms for Highly Efficient, Load-Balanced, and Scalable Molecular Simulation. *J. Chem. Theory Comput.* **2008**, *4*, 435−447.

(28) Johnson, J. K.; Zollweg, J. A.; Gubbins, K. E. The Lennard-Jones equation of state revisited. *Mol. Phys.* **1993**, *78*, 591−618.

(29) Penn, R. L.; Banfield, J. F. Imperfect Oriented Attachment: Dislocation Generation in Defect-Free Nanocrystals. *Science* **1998**, *281*, 969−971.

(30) Steinhart, M.; Senz, S.; Wehrspohn, R. B.; Gösele, U.; Wendorff, J. H. Curvature-Directed Crystallization of Poly(vinylidene difluoride) in Nanotube Walls. *Macromolecules* **2003**, *36*, 3646−3651.

(31) Tretinnikov, O. N.; Ikada, Y. Dynamic Wetting and Contact Angle Hysteresis of Polymer Surfaces Studied with the Modified Wilhelmy Balance Method. *Langmuir* **1994**, *10*, 1606−1614.

(32) Wang, X. Q. Phases of the Au(100) surface reconstruction. *Phys. Rev. Lett.* **1991**, *67*, 3547.

(33) Binnig, G.; Rohrer, H.; Gerber, C.; Weibel, E. 7Œ7 reconstruction on Si (111) resolved in real space. *Phys. Rev. Lett.* **1983**, *50*, 120.

(34) Wolansky, G.; Marmur, A. The Actual Contact Angle on a Heterogeneous Rough Surface in Three Dimensions. *Langmuir* **1998**, *14*, 5292−5297.

(35) Kirkwood, J. G.; Buff, F. P. The Statistical Mechanical Theory of Surface Tension. *J. Chem. Phys.* **1949**, *17*, 338−343.

(36) Nijmeijer, M. J. P.; Bruin, C.; van Woerkom, A. B.; Bakker, A. F.; van Leeuwen, J. M. J. Molecular dynamics of the surface tension of a drop. *J. Chem. Phys.* **1992**, *96*, 565−576.

DOI: 10.1021/acs.langmuir.5b03925
Langmuir 2016, 32, 316−321